Research Square

Preprints are preliminary reports that have not undergone peer review.
They should not be considered conclusive, used to inform clinical practice,
or referenced by the media as validated information.

Formation and Evolution of Shallow Subsurface Defects beneath Urban Roads in Coastal Soft Ground

Hongbo Zhou
SRIBS
Rongxin Zhao
Shanghai Research Institute of Building Sciences Co., Ltd
Yian Wang
Shanghai Research Institute of Building Sciences Co., Ltd
Yinbing Cui
cuiyinbing@sribs.com

Shanghai Research Institute of Building Sciences Co., Ltd

Research Article

Keywords: coastal soft soil, subsurface road defects, multisource evidence, causal attribution, failure pathways

Posted Date: November 13th, 2026

DOI: https://doi.org/10.21203/rs.3.rs-11449981/v1

License: This work is licensed under a Creative Commons Attribution 4.0 International License.
Read Full License

Additional Declarations: No competing interests reported.

Formation and Evolution of Shallow Subsurface Defects beneath Urban Roads in Coastal Soft Ground

Hongbo Zhou[2,3], Rongxin Zhao[1,2],Yian Wang[1,2],Yinbing Cui[1*]

1.Shanghai Research Institute of Building Sciences Co., Ltd., Shanghai 201108, China

2.Shanghai Key Laboratory of Engineering Structure Safety, SRIBS, Shanghai 200032, China

3.Shanghai Research Institute of Building Sciences Group Co., Ltd., Shanghai 201108, China

[*] Corresponding author: cuiyinbing@sribs.com.cn； ORCID: 0009-0001-8127-3304

Abstract

Shallow subsurface defects beneath urban roads in coastal soft ground may result from interacting geological, construction, hydraulic, and loading processes, complicating causal attribution. We investigated ten defects using ground-penetrating radar, borehole and core verification, falling-weight deflectometer testing, drainage-pipeline closed-circuit television inspection, utility detection, historical records, and field reconnaissance. Candidate causes were evaluated case by case using source confirmation, spatial and elevation compatibility, consistency between inferred processes and observed responses, and alternative explanations. One case was repaired before the repeat survey; the remaining nine were compared using anomaly area, depth to the top boundary, equivalent thickness, and defect type. Geological heterogeneity was the best-supported interpretation in four cases. For the remaining cases, the evidence supported, to varying degrees, slope and embankment deformation, disturbance from trenchless construction, internal erosion associated with pipeline damage, or cumulative deformation under prolonged heavy traffic. Between-survey comparisons identified planar expansion, vertical change, type reorganization, relative stability, and mixed change. Divergent responses among indicators showed that an unchanged or reduced anomaly area alone does not demonstrate stabilization. Combining field evidence with previous studies, conditional failure pathways were formulated for differential deformation, construction disturbance, internal erosion, cyclic accumulation of plastic strain, and lateral deformation. A subsurface anomaly does not necessarily imply pavement failure; deterioration also depends on whether the causative process persists, the remaining structural bearing capacity, and the capacity to accommodate differential deformation. At the case scale, these findings support causal attribution, repeat-survey interpretation, and differentiated monitoring and remediation of shallow subsurface road defects in coastal soft ground.

Keywords: coastal soft soil; subsurface road defects; multisource evidence; causal attribution; failure pathways

1 Introduction

Shallow subsurface defects beneath urban roads, including soil loosening, anomalies associated with elevated water content, loss of contact, and cavities, are difficult to detect because they are concealed, develop through complex processes, and often produce delayed surface manifestations. During the early stages of development, the overlying pavement may remain largely intact. Continued loss of soil particles, densification, or accumulation of deformation can gradually reduce the effective support beneath the pavement, resulting in increased deflection, rutting, cracking, and settlement. Under certain conditions, these processes may eventually cause localized pavement collapse [1, 3]. Coastal areas underlain by soft soils commonly contain shallow artificial fill, backfilled creeks, paleochannels, and weak sedimentary strata, together with dense networks of subsurface utilities. Geological susceptibility, construction disturbance, hydraulic action, and traffic loading may therefore overlap spatially, making it difficult to attribute an individual defect to a single factor.

Previous studies have investigated permanent deformation of soft ground under cyclic loading [4, 5], the loss of soil particles and development of voids around damaged pipelines [6, 8], ground disturbance, ground loss, and surface settlement caused by trenchless construction [9, 10], and hydromechanical changes in slopes subjected to rainfall infiltration [11, 12]. These studies provide a physical basis for understanding several representative failure processes. However, most have examined individual factors through laboratory tests, numerical simulations, or retrospective analyses of failure events. At road sites where geological conditions, underground utilities, construction activities, traffic loading, and hydraulic processes coexist, a transparent and traceable basis for evaluating competing causal explanations remains lacking.

Causal attribution is further complicated by differences in the capabilities, spatial resolutions, and evidential scopes of the available investigation methods. Ground-penetrating radar (GPR) can continuously delineate the location and geometry of subsurface anomalies, but cannot independently determine their physical condition or origin [13, 14]. Borehole investigation and borehole imaging can verify local subsurface conditions, although the resulting evidence is limited by sparse spatial coverage. Falling-weight deflectometer (FWD) testing characterizes the integrated response of the pavement, base course, and subgrade, but cannot isolate a specific causative process [15]. Closed-circuit television (CCTV) inspection, utility detection, and historical records can identify potential causative sources, yet spatial proximity alone does not establish causality [3]. Reliable attribution at field sites therefore requires examination of whether a candidate source is compatible with the defect in terms of horizontal location, elevation, and plausible hydraulic or mechanical pathways. Anomaly geometry, material conditions verified by boreholes, pavement response, and surface deformation must also provide mutually consistent evidence. Alternative explanations with comparable or greater explanatory power should be explicitly examined. Negative evidence, including distant pipeline defects, the absence of relevant utilities within the affected area, or incompatibility between the source elevation and anomaly depth, may be equally important.

A survey conducted at a single time point provides only a snapshot of defect condition. It cannot distinguish residual damage caused by a transient disturbance from a defect that continues to develop because the causative process remains active. Even when the horizontal extent of an anomaly remains unchanged, its top boundary may move toward the ground surface or its thickness may increase. Conversely, an apparent reduction in area may coincide with soil loosening around the anomaly or a change to another anomaly type. Defect activity should therefore be assessed by considering geometric changes, changes in physical condition, persistence of the causative process, and pavement structural response together. Formation of a subsurface defect should also be distinguished from pavement failure. Defect formation concerns the processes responsible for soil loosening, water accumulation, loss of contact, or cavity development. Pavement failure concerns how an existing defect progressively reduces structural support, disrupts deformation compatibility, and eventually manifests as rutting, cracking, settlement, or collapse.

To address these issues, this study investigates ten shallow subsurface road defects in a coastal area underlain by soft soils. The research framework integrates evidence from multiple investigation methods, causal attribution, comparison between the initial and repeat surveys, interpretation of failure mechanisms, and assessment of potential consequences. An evidence chain is first established by combining anomaly geometry, local material conditions, pavement structural response, and external environmental and engineering conditions. Changes in anomaly area, depth to the top boundary, equivalent thickness, and defect type are then compared between the two surveys. Field evidence is subsequently interpreted with reference to previous studies to formulate conditional failure pathways associated with different causative factors and to identify the conditions required for continued defect development. Finally, the changing roles of multiple factors during defect development, the implications for defect management, and the limitations of the available evidence are discussed. The study provides conditional explanations for individual cases. It does not estimate the regional prevalence of different causes, quantify their independent contributions, or calculate the probability of pavement failure.

2 Study area and defect investigation

2.1 Engineering Geological Setting and Road Loading Conditions

The study area lies within a coastal depositional environment. The shallow strata consist mainly of artificial fill, littoral silty deposits, and estuarine clayey deposits. Buried creeks, paleochannels, and fill within former creeks occur locally. Differences among these strata in compressibility, hydraulic conductivity, and water content may cause abrupt changes in subgrade stiffness, differential deformation, and localized water accumulation. These conditions were regarded as background factors that increase susceptibility to defect formation rather than as direct evidence of causation. They were considered evidence for causal attribution in an individual case only when their spatial distribution was consistent with the defect location, material condition, and observed deformation response.

Several road sections lie adjacent to waterways or embankment slopes and may therefore be affected by rainfall infiltration, fluctuations in surface water level, and lateral ground deformation. Drainage, power, and telecommunications utilities are also present beneath the roads, some of which were installed using trenchless construction methods. Other sections have been subjected to prolonged traffic involving heavy vehicles and exhibit rutting, settlement, or repeated pavement repairs. Because continuous records of groundwater level and pore water pressure, together with complete axle load data, were unavailable, hydraulic action and traffic loading were considered only as candidate causative factors. Their relevance was evaluated separately for each case by examining spatial correspondence, anomaly characteristics, changes between the initial and repeat surveys, and FWD responses.

The study included ten sites at which shallow subsurface defects beneath roads had previously been identified (Fig. 1). Pavement rehabilitation at C06 had been completed before the repeat survey. Because this intervention altered the original defect and its boundary conditions, C06 was used only to characterize changes in subsurface conditions after intervention. The remaining nine cases were included in the analyses of causal attribution and defect evolution. All sites were selected from previously identified defects rather than through probability sampling. They therefore cannot be used to infer the density of subsurface defects beneath roads or the relative frequency of different causes across the study area.



Fig. 1 Location of the study area and spatial distribution of the ten investigated defect sites

2.2 Investigation methods and evaluation criteria

Imaging with ground-penetrating radar (GPR) was conducted in two dimensions along 90 survey lines, with a total length of approximately 4,109.2 m. The surveys were used to delineate the horizontal extent and upper and lower boundaries of the subsurface anomalies. Verification was conducted using 26 boreholes. Borehole imaging and pavement coring were also performed to confirm cavities, loss of contact, soil loosening, locally elevated water content, and the configuration of the pavement layers. Falling-weight deflectometer (FWD) measurements were collected at 116 locations to characterize the integrated structural response of the pavement. Closed-circuit television (CCTV) inspection was conducted along approximately 992.1 m of drainage pipes to identify breakage, deformation, misalignment, and joint separation. Utility detection, historical geological and construction records, and field reconnaissance were used to examine buried creeks, paleochannels, utility crossings, surface settlement, cracking, rutting, and lateral slope displacement. The evidential role and limitations of each method are summarized in Table 1.

Representative field operations are shown in Fig. 2. GPR surveying provided continuous profiles of subsurface reflections, whereas borehole verification and pavement coring supplied local observations of subsurface conditions and pavement-layer composition. The recovered core from C03 illustrates the material evidence used to interpret the pavement structure. These complementary observations linked geophysical anomalies to local physical conditions; individual photographs or core samples alone were not used to infer the full extent or cause of a defect.



Fig. 2 Field investigation of shallow subsurface road defects: (**a**) GPR surveying; (**b**) borehole verification; (**c**) pavement coring; and (**d**) a recovered pavement core from C03

The investigation was organized into three stages. These consisted of preliminary reconnaissance, screening of candidate factors, and field verification (Fig. 3). Repeat GPR surveys and field reconnaissance were first used to confirm the anomalies and characterize the surrounding conditions. Underground utilities, geological conditions, construction disturbance, traffic loading, and slope deformation were considered in parallel as candidate explanations. Preliminary interpretations based on these lines of evidence were then evaluated against the results of borehole investigation, borehole imaging, pavement coring, and FWD testing. This workflow represents the sequence in which evidence was collected and verified. It does not represent the temporal sequence of defect development.

Five criteria were used for causal attribution. The first assessed whether the candidate causative source was demonstrably present. The second considered, when temporal information was available, whether the candidate factor preceded defect formation or remained active during subsequent development. The third examined the compatibility between the source and the defect with respect to horizontal location, elevation of action, and plausible hydraulic or mechanical pathways. The fourth assessed whether anomaly geometry, material conditions confirmed by boreholes, pavement response, and surface deformation were consistent with the proposed mechanism. The fifth considered whether any alternative factor had comparable or greater explanatory power. A candidate factor was identified as the primary explanation with the strongest evidential support only when a coherent chain could be established from the causative source, through a plausible action pathway, to the observed defect response. Factors that promoted the development of an existing defect were classified as contributory factors. Conditions that increased ground susceptibility but could not independently explain the observed defect geometry were classified as predisposing conditions. Confidence in the attribution was reduced when temporal information or evidence of the relevant action pathway was unavailable.

Table 1 Multisource investigation methods and their evidential roles.

Investigation method	Principal information obtained	Principal evidential role	Limitations
GPR	Anomaly extent, burial depth, and continuity	Delineates anomalies and guides the placement of verification boreholes	Affected by material composition, water content, and interference at the site
Borehole investigation and borehole imaging	Cavities, loss of contact, soil loosening, and locally elevated water content	Verifies the physical condition and type of anomalies at target locations	Discrete sampling points cannot fully define defect boundaries
Pavement coring	Composition, thickness, and integrity of pavement layers	Supports interpretation of pavement deflection and loss of contact	Represents conditions only at the coring location
FWD testing	Deflection response of the pavement structure	Evaluates the structural response and its spatial variation	Affected by structural composition, defect depth, and measurement location
CCTV inspection of drainage pipelines	Type and grade of pipeline defects	Identifies potential sources of water and soil loss	A pipeline defect does not by itself establish causation
Subsurface utility detection	Utility location, burial depth, and alignment	Verifies horizontal location and relevant elevation	Some elevation and construction records are unavailable
Historical records and field reconnaissance	Geological setting, construction disturbance, and surface deformation	Identifies candidate factors and supplements evidence of the relevant processes	Data completeness and temporal precision are inconsistent

Four geometric descriptors were used to compare the initial and repeat surveys. These comprised the horizontal anomaly area (A), depth to the top boundary (z_t), depth to the lower boundary (z_b), and equivalent thickness (H). Equivalent thickness was calculated as:

$$H = z_b - z_t$$

For anomalies of the same type, the relative changes in area and equivalent thickness, together with the upward displacement of the top boundary, were calculated as follows:

$$R_A = (A_1 - A_0)/A_0 \times 100\%$$

$$R_H = (H_1 - H_0)/H_0 \times 100\%$$

$$U_t = z_{t,0} - z_{t,1}$$

where subscripts 0 and 1 denote the initial and repeat surveys, respectively. A positive value of (U_t) indicates movement of the top boundary toward the ground surface. Because anomalies of different types may overlap, the areas of cavities, zones with loss of contact, loosened soil, and anomalies associated with elevated water content were not summed directly. When the interpreted anomaly type changed between surveys or the survey records were inconsistent, only the apparent change was described. Changes in volume across anomaly types were not calculated. Annual rates of change were not estimated because information on survey dates, correspondence between survey lines, and errors associated with repeated measurements was incomplete. Small differences were therefore treated only as tentative evidence of a possible trend.

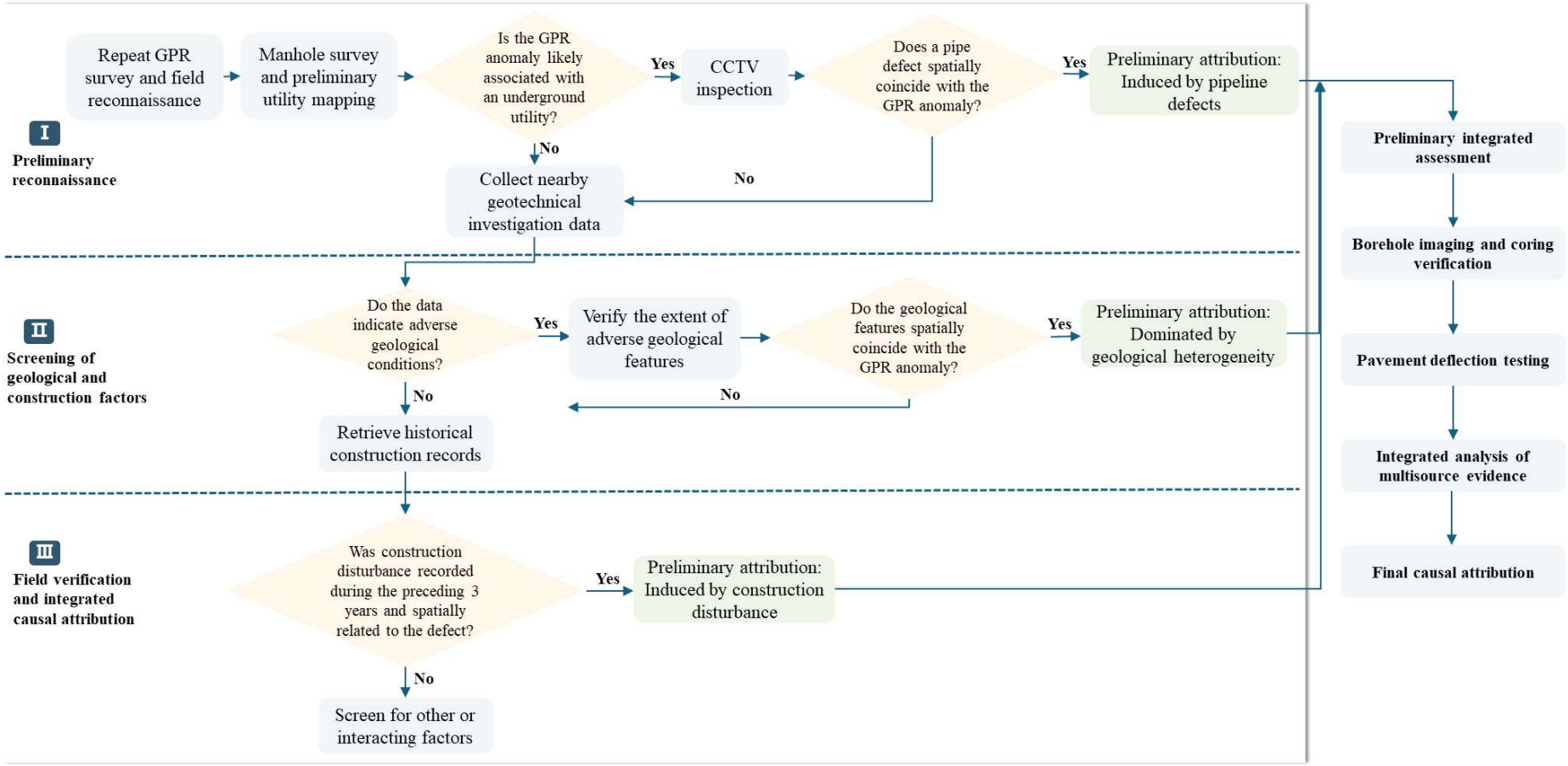


Fig. 3 Workflow for causal screening and field verification of shallow subsurface defects beneath urban roads

2.3 Defect investigation results

The principal findings from the ten investigated defect sites are summarized in Table 2. At the time of the repeat survey, excluding C06, which had undergone rehabilitation, cavities were the dominant anomaly type at four sites. Loss of contact was dominant at one site, an anomaly associated with elevated water content at one site, and severe soil loosening at three sites. Three sites also contained a secondary anomaly type, indicating that classification based on a single category cannot fully characterize the internal configuration of these defects. The top boundaries of the dominant anomalies were located 0.10–0.70 m below the ground surface. All defects were therefore situated within the shallow subsurface zone, where stresses generated by traffic loading and shallow hydraulic processes are likely to have substantial influence.

Figure 4 presents representative repeat-survey GPR profiles for the four defect categories. The highlighted windows show localized reflection changes at C03 (Fig. 4a), banded reflections at C07 (Fig. 4b), a locally undulating reflection band at C04 (Fig. 4c), and irregular shallow reflections at C10 (Fig. 4d). Borehole observations supported the classification by linking radar responses to locally observed physical conditions. Red boxes indicate illustrative anomaly windows rather than measured defect boundaries. Radar patterns alone were not treated as unique indicators of defect type or cause.

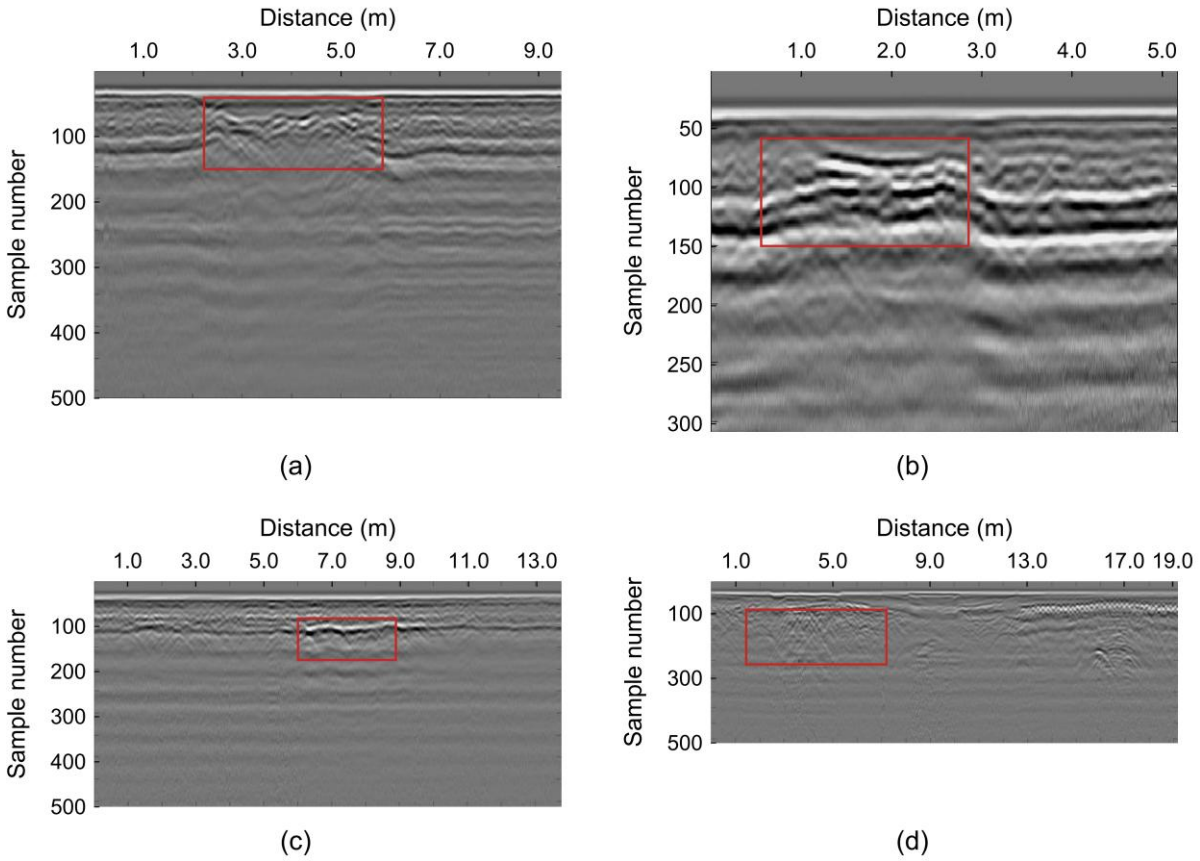


Fig. 4 Representative repeat-survey GPR profiles for (**a**) a cavity at C03, (**b**) an anomaly associated with elevated water content at C07, (**c**) loss of contact at C04, and (**d**) severe soil loosening at C10. Red boxes indicate illustrative anomaly windows, not measured defect boundaries

Table 2 Investigation results and principal environmental evidence for the representative defect sites.

Case	Dominant condition at repeat survey	Geometric parameter (initial→ repeat survey)	Change metric	FWD (mm)	Principal field observations
C01	Cavity	A: 25.2 → 21.3 m² z_t: 0.28 → 0.25 m H: 0.87 → 0.85–0.90 m	R_A: −15.5% U_t: +0.03 m R_H: −2.3% to +3.4%	13.81	A utility installed by trenchless construction crosses the site; Grade 4 breakage of a stormwater branch pipe; discrepancies in the recorded bottom-boundary depth from the repeat survey
C02	Cavity and moderate soil loosening	A: 9.09 → 2.20 m² z_t: 0.25 → 0.35 m H: 0.45 → 0.55 m	R_A: −75.8% U_t: −0.10 m R_H: +22.2%	67.36	An additional 11.8 m² zone of moderate soil loosening; no persistent nearby pipe damage sufficient to explain the defect
C03	Cavity	A: 10.1 → 10.1 m² z_t: 0.75 → 0.60 m H: 0.20 → 0.35 m	R_A: 0.0% U_t: +0.15 m R_H: +75.0%	14.91	A pipeline defect lies approximately 25.5 m from the anomaly; heterogeneous ground occurs within the road corridor
C04	Loss of contact and severe soil loosening	A: 6.0 → 6.0 m² z_t: 0.40 → 0.40 m H: 0.20 → 0.20 m	R_A: 0.0% U_t: 0.00 m R_H: 0.0%	35.6	An additional 10.2 m² zone of severe soil loosening; historical records and boreholes jointly indicate a buried creek
C05	Cavity	A: 1.1 → 1.1 m² z_t: 0.65–0.70 m H: 0.10 → 0.30 m	R_A: 0.0% U_t: — R_H: +200.0%	91.42	A nearby buried creek and paleochannel; discrepancies in the recorded depths and distances from the pipeline
C06	Rehabilitation intervention	—	—	—	The road was rehabilitated before the repeat survey; no anomaly was detected during the repeat survey; excluded from analysis of changes under unaltered site conditions
C07	Anomaly associated with elevated water content	A: 1.0 → 1.0 m² z_t: 0.65 → 0.40 m H: 0.15 → 0.30 m	R_A: 0.0% U_t: +0.25 m R_H: +100.0%	26.95	The horizontal extent was unchanged, but the recorded values indicate upward movement of the top boundary and increased thickness
C08	Severe soil loosening with localized loss of contact	A: 153 → 185 m² z_t: 0.20 → 0.15 m H: 0.50 → 0.60 m	R_A: +21.0% U_t: +0.05 m R_H: +20.0%	84.24	The repeat survey identified 4.9 m² of localized loss of contact; accompanied by lateral embankment displacement and tensile cracks
C09	Severe soil loosening	A: 660 → 777 m² z_t: 0.10 → 0.10 m H: 0.60 → 0.60 m	R_A: +17.7% U_t: 0.00 m R_H: 0.0%	109.36	Prolonged heavy traffic, with pronounced rutting and pavement repairs; no stormwater or wastewater pipe beneath the traffic lane
C10	Severe soil loosening	A: 47.5 → 47.5 m² z_t: 0.30 → 0.30 m H: 0.50 → 0.50 m	R_A: 0.0% U_t: 0.00 m R_H: 0.0%	88.78	Grade 3 breakage and Grade 3 deformation of a stormwater trunk pipe; accompanied by surface settlement and cracking

Comparisons between the initial and repeat surveys showed that changes in horizontal area, equivalent thickness, and depth to the top boundary were not necessarily consistent among the investigated sites. At C02, the cavity area decreased from 9.09 to 2.20 m², corresponding to (R_A=-75.8%), the largest apparent reduction in cavity area among the investigated cases. In contrast, the equivalent thickness increased from 0.45 to 0.55 m (R_H=22.2%), while the depth to the top boundary increased from 0.25 to 0.35 m (U_t=-0.10m). An additional 11.8 m² zone of general soil loosening was identified during the repeat survey. The change in area was calculated only for the cavity and did not include the newly identified loosened zone. It therefore does not represent a 75.8% reduction in the overall extent of the defect.

C08 and C09 were characterized primarily by horizontal expansion. At C08, the area of severe soil loosening increased from 153 to 185 m² (R_A=21.0%), while the equivalent thickness increased from 0.50 to

0.60 m (R_H=20.0%). The top boundary also moved 0.05 m toward the ground surface. In addition, a localized zone with loss of contact, covering 4.9 m², was identified during the repeat survey. At C09, the area of severe soil loosening increased from 660 to 777 m² (R_A=17.7%), whereas neither the equivalent thickness nor the recorded depth to the top boundary changed. The difference between the two surveys at this site was therefore concentrated mainly in the horizontal extent.

The principal differences at C03, C05, and C07 occurred in the vertical geometric indicators. At C03, the cavity area remained unchanged at 10.1 m², whereas its equivalent thickness increased from 0.20 to 0.35 m (R_H=75.0%). The top boundary also moved 0.15 m toward the ground surface. Similarly, the anomaly associated with elevated water content at C07 retained an area of 1.0 m², but its equivalent thickness increased from 0.15 to 0.30 m (R_H=100.0%), and its top boundary moved 0.25 m toward the ground surface. Thus, although the horizontal areas at these two sites remained unchanged, substantial differences were recorded in their vertical boundaries. At C05, the equivalent thickness increased from 0.10 to 0.30 m, corresponding to (R_H=200.0%), the largest relative change among the investigated cases. However, the absolute increase was only 0.20 m, and the large relative value was partly attributable to the small initial thickness. Furthermore, the available records did not clearly distinguish the depths to the top boundary in the two surveys, preventing a reliable calculation of (U_t). C05 can therefore be interpreted only as exhibiting an apparent difference in thickness. The direction of vertical boundary movement cannot be determined.

Changes at the remaining sites were comparatively limited. At C01, the cavity area decreased from 25.2 to 21.3 m² (R_A=-15.5%). However, inconsistencies in the records of the bottom boundary from the repeat survey prevented determination of the direction of vertical change. At C04 and C10, both (R_A) and (U_t) were zero, and no major geometric changes were identified under the available survey conditions. Because C06 had undergone pavement rehabilitation before the repeat survey and no anomaly was subsequently identified, it was excluded from the comparison of changes under unaltered site conditions. Representative FWD values for all sites are reported in Table 2. Their spatial differences were used to characterize pavement structural responses rather than as direct evidence of defect causation.

3 Causal attribution of subsurface defects

The candidate causes were divided into natural and anthropogenic factors. Natural factors included weak and heterogeneous ground, buried creeks and paleochannels, and deformation of slopes and embankments. Anthropogenic factors included disturbance from trenchless construction, damage to drainage pipelines, and cyclic traffic loading. This classification was used only to organize the candidate explanations. Attribution at the level of individual cases remained based on an evidence chain connecting the causative source, action pathway, defect response, and alternative explanations (Table 3).

3.1 Causal attribution under natural and anthropogenic factors

Cases C03, C04, C05, C07, and C08 were primarily associated with natural factors. C03, C04, C05, and C07 coincided spatially with buried creeks, paleochannels, fill within former creeks, or former open creeks. For these cases, either no persistent anthropogenic source was identified nearby or the available anthropogenic evidence had limited explanatory power. At C04, both historical records and borehole evidence confirmed the presence of a buried creek, whereas the pipeline defect did not overlap spatially with the subsurface anomaly. The evidence supporting the geological explanation was therefore comparatively complete. At C05, discrepancies in the recorded anomaly depths and distances from the pipeline mean that a possible contribution from pipeline damage cannot be excluded. At C07, the anomaly area remained approximately 1.0 m² in both surveys, with no detectable expansion in its horizontal extent. However, the recorded values of (R_H=100.0%) and (U_t=0.25m) indicated a substantial apparent vertical change. Consequently, only the horizontal extent can be regarded as relatively stable. The overall defect condition should not be classified as stable. At C08, the spatial correspondence among soil loosening, localized loss of contact, lateral displacement of the embankment, and tensile cracking provided mutually consistent evidence. Deformation of the slope and embankment was therefore among the explanations with the strongest evidential support. Nevertheless, the absence of continuous monitoring of displacement and pore water pressure prevented identification of the specific triggering period.

Cases C01, C02, C09, and C10 were primarily associated with anthropogenic factors. At C01 and C02, utility lines installed by trenchless construction crossed the affected zones, and the localized cavities were compatible with the expected extent of construction disturbance. Disturbance from trenchless construction was therefore considered the most plausible initiating factor. At C01, subsequent hydraulic effects may also have developed because of damage to a branch drainage pipe. At C10, the spatial correspondence among the pipeline defect, loosened zone, FWD gradient within the road section, and surface settlement provided strong support for internal erosion associated with pipeline damage. However, reverse causality could not be fully excluded because ground deformation may have preceded and contributed to the pipeline damage. At C09, severe soil loosening was concentrated beneath a traffic lane subjected to prolonged loading from heavy vehicles and was accompanied by rutting and repeated pavement repairs. Cyclic traffic loading was therefore considered the most plausible persistent driving factor. Because axle load spectra, water content measurements, and a control road section were unavailable, the evidential support for this attribution was weaker than that for C04, C08, and C10.

C06 had undergone pavement rehabilitation before the repeat survey. The absence of a detectable anomaly after rehabilitation indicates only that the subsurface condition changed following intervention. It cannot be used to infer the original cause retrospectively. C06 was therefore excluded from the assessment of causal composition across cases and from the comparison of changes at sites without intervention.

Table 3 Evidence chains and results of causal attribution for representative subsurface defects.

Case	Principal defect type	Principal best-supported causal interpretation	Principal evidence	Limitations of attribution	Attribution result
C01	Cavity	Disturbance from trenchless construction	A utility installed by trenchless construction crosses the defect zone; the localized cavity is spatially consistent with the utility alignment	Construction records are incomplete; breakage of a branch pipe may have contributed to subsequent water and soil loss	The construction-related explanation is best supported, with a possible concurrent contribution from pipe damage; moderate evidential support
C02	Cavity and moderate soil loosening	Disturbance from trenchless construction	A utility installed by trenchless construction crosses the defect zone; localized anomalies occur along the utility alignment	Complete construction records are unavailable; reduction of the cavity area coincided with soil loosening	A construction-related explanation is reasonably supported; moderate evidential support
C03	Cavity	Buried creek and associated geological heterogeneity	The defect coincides spatially with heterogeneous strata, and its geometry is compatible with differential deformation	The pipeline defect lies approximately 25.5 m from the anomaly; continuous stratigraphic profiles are unavailable	An explanation involving geological heterogeneity is best supported; moderate evidential support
C04	Loss of contact and severe soil loosening	Settlement of buried-creek fill	Historical records and boreholes jointly confirm a buried creek; the defect coincides with its location	The pipeline defect does not overlap the subsurface anomaly	The explanation involving a buried creek has relatively strong evidential support
C05	Cavity	Settlement associated with a buried creek and paleochannel	Boreholes and historical records identify fill within a former creek and a paleochannel; their locations are spatially consistent with the defect	Recorded depths and pipeline distances are inconsistent, and a contribution from pipe damage cannot be fully excluded	An explanation involving adverse geological conditions is best supported; moderate evidential support
C06	Original anomaly associated with elevated water content	Undetermined	No anomaly was detected after pavement rehabilitation	Independent evidence of the causative source before intervention is unavailable; the post-intervention result cannot be used to infer the original cause	Evidence is insufficient for definitive attribution
C07	Anomaly associated with elevated water content	Former open creek and heterogeneous ground	A former open creek is located nearby; no subsurface utility was detected in the surrounding area; the elevated water content is compatible with localized water accumulation	The anomaly extent was essentially unchanged between the two surveys	An explanation involving the geological and hydrological setting is reasonably supported; moderate evidential support
C08	Severe soil loosening and localized loss of contact	Slope and embankment deformation	Lateral embankment displacement and tensile cracks coincide spatially with extensive soil loosening and localized loss of contact	Concurrent records of rainfall, pore pressure, and continuous displacement are unavailable; reverse causality cannot be fully excluded	An explanation involving slope and embankment deformation has relatively strong evidential support
C09	Severe soil loosening	Prolonged heavy traffic	Extensive soil loosening beneath the traffic lane, rutting, and a relatively high representative FWD value; no stormwater or wastewater pipe lies beneath the lane	Axle-load spectra, water-content measurements, and a control road section are unavailable; effects of geological conditions cannot be fully excluded	An explanation involving traffic loading is reasonably supported; moderate evidential support
C10	Severe soil loosening	Damage to a stormwater trunk pipe	Pipe damage, the loosened zone, the deflection gradient, settlement, and cracking exhibit consistent spatial correspondence	Monitoring of hydraulic head and particle loss is unavailable; whether pre-existing ground deformation contributed to pipe damage remains unclear	An explanation involving internal erosion associated with pipe damage has relatively strong evidential support

3.2 Patterns of causal attribution across cases

Comparison across cases showed that spatial proximity alone is useful only for identifying candidate explanations. It provides stronger discriminatory evidence only when the location and relevant elevation of the causative source, the inferred action or migration pathway, defect geometry, and pavement response are mutually compatible. Although pipeline defects were identified near C03 and C04, their considerable distance from the subsurface anomalies or lack of spatial overlap weakened explanations involving the pipelines. By contrast, the pipeline defects at C10 were spatially consistent with the loosened zone, the FWD gradient within the road section, and the observed surface deformation. These observations formed a more coherent evidence chain.

Defect type and FWD response can indicate compatibility with a proposed mechanism but cannot independently establish causation. Localized cavities may result from construction disturbance, differential settlement, or soil loss. Extensive shallow soil loosening may be associated with traffic loading, geological heterogeneity, or embankment deformation. Negative evidence can reduce the plausibility of a candidate explanation but cannot establish the complete absence of the corresponding factor. The absence of a detected utility or pipeline defect provides strong negative evidence only when the investigation coverage and data completeness are sufficient.

Different factors may also play distinct roles during defect initiation and subsequent development. Soft soils, buried creeks, and paleochannels generally act as predisposing conditions. Construction disturbance, pipeline damage, and slope displacement may initiate localized defects. Persistent leakage, cyclic loading, and continuing slope deformation may sustain their development. Intense rainfall, variations in water levels within pipelines, or additional loading may further destabilize existing weak zones. The distinction between natural and anthropogenic factors therefore identifies the origin of the candidate factors. It does not imply that a single factor governs the entire development process.

4 Stage-specific changes in subsurface defects and potential failure mechanisms

4.1 Stage-specific changes identified by comparison of the initial and repeat surveys

Excluding C06, where pavement rehabilitation had been completed before the repeat survey, nine cases were available for comparison. Based on the relative changes in anomaly area (R_A) and equivalent thickness (R_H), the upward displacement of the top boundary (U_t), and changes in anomaly composition, the observed differences were classified into six principal patterns: simultaneous horizontal and vertical expansion, predominantly horizontal expansion, predominantly vertical change, area contraction accompanied by a change in anomaly composition, relative geometric stability, and mixed or indeterminate change (Table 4). These categories describe the apparent differences between two discrete surveys. They should not be interpreted as evidence of a continuously monitored evolutionary process or used to estimate rates of change.

Table 4 Patterns of apparent change in subsurface defects identified by comparison of the initial and repeat surveys.

Principal pattern of change	Principal diagnostic features	Representative cases
Simultaneous horizontal and vertical expansion	R_A >0 and R_H >0, accompanied by upward movement of the top boundary	C08
Predominantly horizontal expansion	R_A >0, with no discernible change in the vertical indicators	C09
Predominantly vertical change	The recorded area was unchanged, but thickness increased and/or the top boundary moved upward	C03, C07
Area contraction accompanied by a change in anomaly composition	The area of the dominant cavity decreased, accompanied by increased thickness or an anomaly of another type	C02
Relative geometric stability	No discernible changes in R_A, R_H, or U_t	C04, C10
Mixed or indeterminate change	Indicators changed in inconsistent directions, or discrepancies existed in the original records	C01, C05

At C08, RA, RH, and Ut were 21.0%, 20.0%, and 0.05 m, respectively. The increase in horizontal extent and thickness, together with the upward movement of the top boundary, indicates simultaneous horizontal and vertical expansion. At C09, R_A was 17.7%, whereas both R_H and U_t were zero. The observed

change was therefore dominated by horizontal expansion. The recorded anomaly areas at C03 and C07 remained unchanged, but both cases exhibited an increase in thickness and upward movement of the top boundary. These results demonstrate that an unchanged horizontal boundary does not necessarily indicate overall geometric stability. At C02, the cavity area decreased by 75.8%, whereas its equivalent thickness increased by 22.2%. In addition, a zone of moderate soil loosening covering 11.8 m² was identified during the repeat survey. This case was therefore characterized by both cavity contraction and a change in anomaly composition. However, these contrasting changes do not demonstrate that the cavity dissipated or was directly transformed into loosened soil. No detectable changes in the three geometric descriptors were recorded at C04 or C10. These two cases were therefore classified as relatively stable in geometric terms during the observation interval. Loss of contact and severe soil loosening coexisted at C04, but the available evidence does not establish a transition between these anomaly types. At C01, the recorded changes in anomaly area, depth to the top boundary, and equivalent thickness were inconsistent. The records of the bottom boundary from the repeat survey also contained discrepancies. At C05, an increase in equivalent thickness was recorded, but the depths to the top boundary could not be reliably matched between the two surveys. The direction of vertical migration therefore could not be determined. Accordingly, C01 and C05 were classified as cases with mixed or indeterminate changes.

Overall, changes in horizontal extent, vertical thickness, and the position of the top boundary were not necessarily synchronous. Vertical changes may occur even when the anomaly area remains unchanged. Conversely, a reduction in area may coincide with an increase in thickness or a change in anomaly composition. Defect condition should therefore be evaluated jointly using RA, RH, Ut, and anomaly type, rather than inferred from area change alone. Relative geometric stability indicates only that no discernible change was identified under the available survey resolution, spatial comparability, and interpretation conditions. It does not demonstrate that the causative process has ceased.

4.2 Potential development pathways and failure mechanisms under different causative conditions

Chapter 3 identified the most plausible causes of the individual cases from multiple sources of field evidence, while Section 4.1 characterized the apparent differences between the initial and repeat surveys. Building on these findings, this section examines the processes through which different causative factors may degrade ground support and induce pavement responses. Figures 5–9 present conceptual development pathways constrained by the available field evidence. They are not intended to reconstruct the complete history of any individual case. The investigation identified the distribution of subsurface anomalies, external causative conditions, and pavement responses, but did not continuously capture soil deformation, particle migration, or internal stress redistribution. The intermediate processes illustrated in these figures are therefore interpreted from established principles of engineering geology and pavement engineering and should not be regarded as having been directly verified in their entirety.

4.2.1 Differential deformation under adverse geological conditions

The subsurface anomalies at C03, C04, C05, and C07 spatially coincide with soft and heterogeneous ground associated with buried creeks, paleochannels, creek fills, or former open creeks. Pronounced variations in soil composition, density, and compressibility within these deposits provide the geological basis for localized incompatible deformation.

As illustrated in Fig. 5, soft deposits generally undergo greater compression under overlying loads than adjacent, more competent ground. This contrast can induce differential settlement and local bending of the pavement structure [16]. As deformation accumulates, localized separation may develop between the base course and the underlying ground. The initially continuous support is consequently replaced by nonuniform support, which may manifest as soil loosening, localized loss of contact, and pavement deformation [17]. Where groundwater movement or pathways for particle migration are also present, the deterioration in local support may progress further. Differential deformation can therefore explain the spatial distribution of these defects and the observed changes in support conditions, but it cannot independently account for every cavity or anomaly characterized by water enrichment.

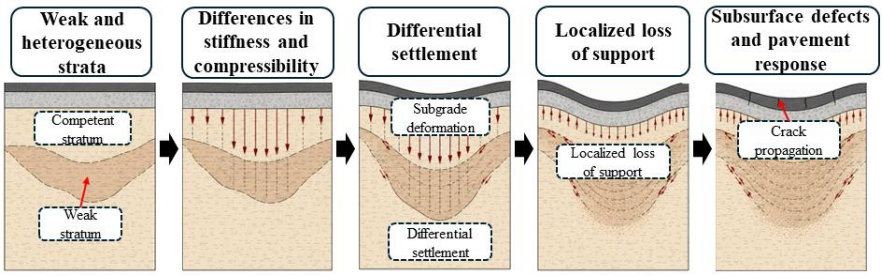


Fig. 5 Conceptual development pathway of shallow subsurface defects under adverse geological conditions

The spatial relationships between the geological features and the anomalies support this mechanistic interpretation, although the available data do not directly record the progressive development of differential settlement. At C07, the horizontal extent remained unchanged between the two surveys, whereas the recorded results indicated upward movement of the top boundary and an increase in equivalent thickness. The horizontal extent can therefore be regarded as relatively stable, but whether the recorded vertical differences exceed the uncertainties associated with survey measurement and interpretation requires further verification. This case indicates that adverse geological conditions may constitute a persistent background of susceptibility without necessarily causing continuous defect expansion over a short period. Figure 5 therefore represents a potential development pathway rather than a common sequence that has been fully experienced by all four cases.

4.2.2 Slope and embankment deformation without toe support

C08 is located along the exposed side of the road, where the defect distribution corresponds spatially to an embankment slope lacking effective toe support. Extensive soil loosening was accompanied by lateral compression, tensile cracking, and relatively high pavement deflection. These observations indicate that the defect may be governed not only by vertical compression but also by lateral deformation of the slope.

As shown in Fig. 6, the absence of toe support provides limited lateral restraint to a weak embankment adjacent to an exposed slope. Under self-weight and traffic loading, the soil on the exposed side may move outward, promoting shallow shear deformation and settlement along the outer edge of the slope crest. As lateral displacement and vertical deformation accumulate, tensile cracks develop near the crest. Support beneath the outer portion of the road is progressively reduced, eventually producing shoulder settlement, longitudinal pavement cracking, and localized deformation.

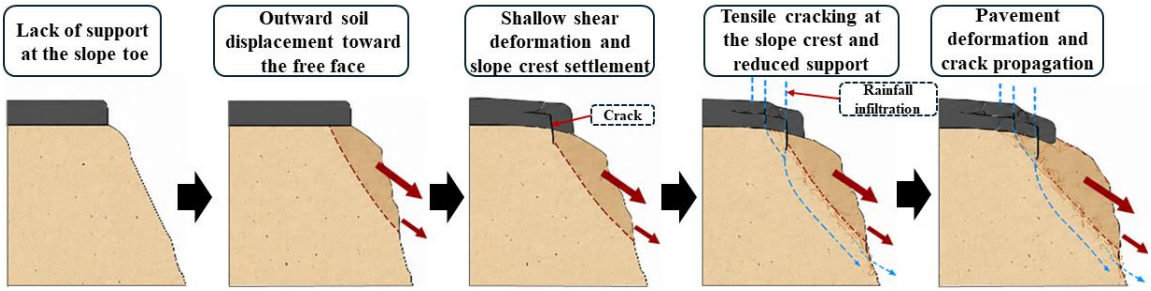


Fig. 6 Conceptual development pathway of shallow subsurface defects induced by slope and embankment deformation

Rainfall infiltration is not considered the initiating cause in this pathway. Once cracks have formed near the slope crest, rainfall may enter the slope through these preferential pathways, promote localized softening and fine particle migration, and thereby amplify the existing deformation [11, 12]. At C08, the spatial correspondence among the loosened zone, lateral compression, tensile cracking, and pavement deflection supports this interpretation. However, the absence of continuous displacement, groundwater level, and pore water pressure monitoring prevents direct reconstruction of the complete deformation sequence and quantitative separation of the contributions from inadequate toe restraint and rainfall infiltration.

4.2.3 Disturbance induced by trenchless construction

The subsurface anomalies at C01 and C02 intersect the alignments of utilities installed using trenchless methods. This spatial relationship provides an important basis for attributing the defects to construction

disturbance. Horizontal directional drilling involves pilot drilling, bore enlargement, and pipe pullback. Its effects may extend beyond the space occupied by the installed pipe and may include disturbance of the bore wall, interaction with drilling fluid, and localized overexcavation.

As illustrated in Fig. 7, rotation of the drilling assembly and the reaming and pullback processes can disturb the surrounding soil and locally remould its original structure. Inadequate control of bore enlargement, insufficient filling by drilling fluid, or incomplete closure of the bore may leave irregular annular gaps and localized loosened zones around the installed pipe. These residual disturbances do not necessarily cause immediate pavement damage. Subsequent adjustment under overlying loads and variations in moisture conditions may nevertheless reduce support beneath the base course and eventually contribute to settlement or cracking [9, 10].

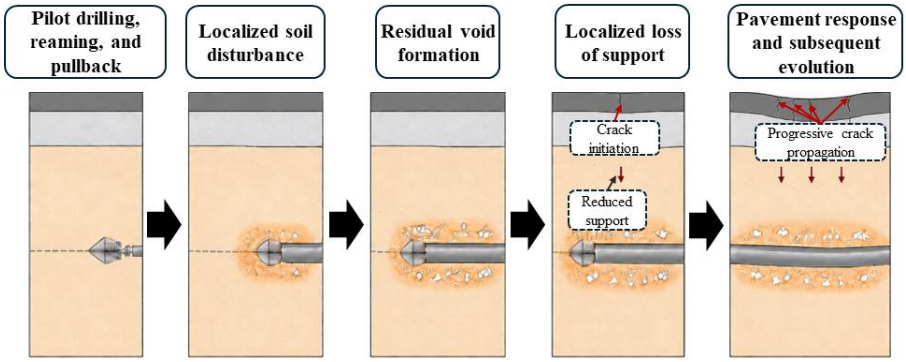


Fig. 7 Conceptual development pathway of shallow subsurface defects induced by trenchless construction

The deflections measured at C01 and C02 were generally within normal or specified limits, indicating that the overall load-bearing response of the two road sections had not undergone marked deterioration at the time of investigation. The support degradation and pavement responses shown in the later stages of Fig. 7 therefore represent potential consequences of continued development rather than conditions already reached at both sites. Damage to a branch stormwater pipe near C01 may have contributed to subsequent development. By contrast, the pipeline defect identified near C02 was too far from the anomaly to constitute its primary cause. Because no comparative surveys before and after construction or records of reaming parameters and drilling fluid pressure were available, the extent of the residual voids cannot be determined directly from the existing evidence.

4.2.4 Pipeline damage and internal erosion

The stormwater main at C10 exhibited deformation and damage. The affected section broadly coincided with the subsurface loosened zone and was accompanied by transverse variations in pavement deflection, surface settlement, and pavement cracking. Unlike the conventional mechanism involving leakage from a pressurized pipe, the interpretation for C10 assumes that external groundwater entered a drainage pipe that was only partially filled or essentially empty.

As shown in Fig. 8, when the groundwater level is above the pipe and the pipe is not flowing full, cracks in the pipe wall can form inward seepage pathways from the surrounding ground. Groundwater enters the pipe through these openings and transports fine particles from the surrounding soil into the pipe. Continued particle loss progressively loosens the soil above the damaged section, allowing localized voiding to propagate upward from the pipe defect [6, 8]. When the affected zone approaches the underside of the base course, pavement support is reduced, potentially leading to flexural deformation, settlement, and cracking.

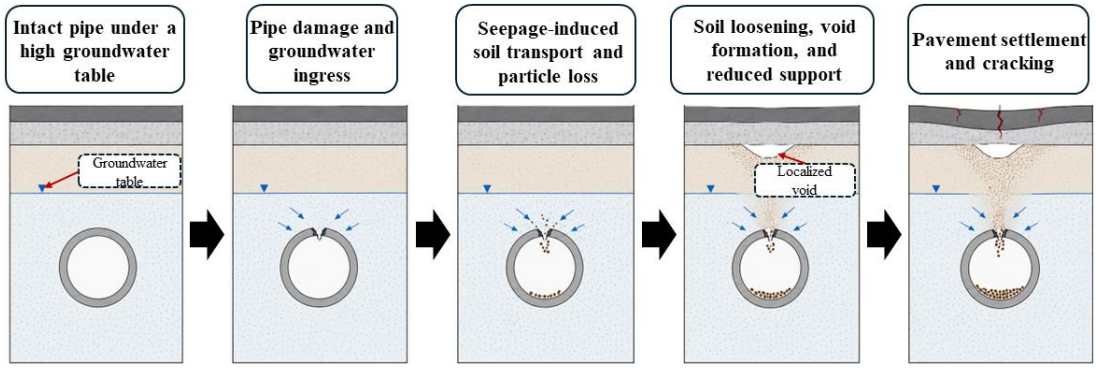


Fig. 8 Conceptual development pathway of seepage erosion and pavement response associated with pipeline damage

The spatial correspondence among pipeline damage, subsurface loosening, the deflection gradient, and surface damage provides a relatively coherent evidence chain for internal erosion at C10. However, the hydraulic head difference between the ground and the pipe, seepage discharge, and rate of particle loss were not continuously monitored. Although the inferred direction of groundwater and soil migration is hydraulically plausible, its rate of development and spatial extent remain mechanistic inferences and cannot be quantitatively reconstructed from the available data.

4.2.5 Cyclic traffic loading

Severe soil loosening at C09 was concentrated beneath a traffic lane subjected to prolonged heavy vehicle loading. The site also exhibited relatively large pavement deflections, pronounced rutting, and repeated repairs. No utilities were identified beneath the principal defect zone, reducing the plausibility of pipeline damage or construction disturbance as the primary cause. The spatial distribution of the defect and the associated pavement response are more consistent with cumulative deformation under cyclic traffic loading.

As illustrated in Fig. 9, repeated vehicle loading along similar wheel paths can progressively accumulate irreversible plastic strain in the subgrade. Within initially weak zones, cyclic stresses induce particle rearrangement and nonuniform densification, which further increase spatial variations in ground stiffness. As the deformation zone expands, support beneath the base course becomes increasingly uneven, and stress concentrations develop along the margins of the weakened zone. The pavement may consequently exhibit a settlement trough, rutting, and fatigue cracking. This pathway represents a long-term cumulative response rather than sudden failure caused by a single overload event [4, 5].

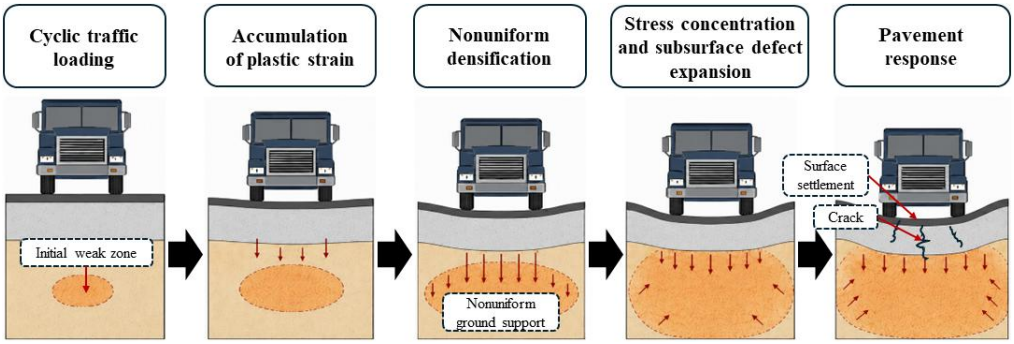


Fig. 9 Conceptual development pathway of a pre-existing weak zone under cyclic traffic loading

The correspondence among soil loosening, elevated deflection, and rutting at C09 supports the interpretation that prolonged heavy traffic was the principal causative factor. Nevertheless, traffic volume, vehicle axle-load spectra, and the dynamic response of the subgrade were not monitored. The available evidence is therefore insufficient to determine either the rate of plastic strain accumulation or the threshold for pavement damage. Initial heterogeneity of the ground may also have influenced the location and severity of cyclic deformation and cannot be fully excluded.

4.3 Potential for self-limitation and conditions for continued development

In this study, self-limitation does not imply that a subsurface anomaly disappears completely or that the long-term risk has been eliminated. It refers to a reduction in the rate of defect development and a transition to temporary stability after the causative process has weakened. Whether a defect becomes self-limiting depends on the removal of the causative source, closure of the action pathway, persistence of hydraulic or mechanical loading, and the capacity of the remaining ground to provide stable support. Table 5 summarizes the conditional assessment for the different causative factors.

Table 5 Self-limitation potential of subsurface defects under different causative factors.

Causative factor	Potential for temporary self-limitation	Conditions for continued or renewed development	Representative cases
Construction disturbance	May become conditionally self-limiting after construction ceases	Residual voids remain connected to seepage pathways, or nearby pipe damage persists	C01, C02
Geological heterogeneity	May become temporarily stable	Continued compression of weak soil, changes in groundwater conditions, or additional loading	C03, C04, C05, C07
Pipeline damage	Low potential for self-limitation if the defect remains unrepaired	Persistent hydraulic gradients and pathways for particle migration	C10
Traffic loading	Depends on load magnitude and remaining bearing capacity	Continued heavy loading, high water content, or insufficient subgrade bearing capacity	C09
Slope deformation	May temporarily stabilize and subsequently reactivate	Continued slope displacement, rainfall infiltration, or changes in toe conditions	C08

Although the cavity area at C02 decreased, the simultaneous increase in thickness and the occurrence of an additional loosened zone do not support a conclusion that the defect had become self-limiting. Similarly, the limited geometric changes at C04 and C10 indicate only relative stability during the observation interval. They do not demonstrate that the corresponding causative processes had ceased. By contrast, the expansion of severe soil loosening at C08 and C09 suggests that the conditions sustaining defect development may still have been present. Neither the type of causative factor nor the change in anomaly area is therefore sufficient to determine whether a defect is approaching stability. Because only two survey campaigns were available and the relevant monitoring parameters were incomplete, the assessments in Table 5 remain conditional interpretations based on plausible mechanisms. They should not be regarded as verification of long-term stability.

4.4 Stage-specific failure pathways governed by a single dominant factor or interacting factors

The results of causal attribution and the observed changes indicate that defect development depends not only on the type of causative factor but also on the sequence in which different factors act and the functional relationships among them. Figure 10 summarizes two pathways: one governed primarily by a single dominant factor and another involving sequential interaction among multiple factors. In the first pathway, one factor provides a relatively complete explanation of the sequence from ground damage to subsurface defect formation and the associated pavement response. This definition does not exclude the presence of predisposing conditions. In the second pathway, an earlier factor creates a weak zone or an action pathway, after which another factor sustains or amplifies defect development. The mere coexistence of several factors is therefore insufficient to establish an interacting pathway.

In the pathway governed by a single dominant factor, ground compression, seepage erosion, lateral deformation, or cyclic loading causes localized deterioration of ground support. Subsequent development depends on whether the causative source remains active and whether the corresponding action pathway remains open. In a pathway involving interacting factors, loosening caused by construction, heterogeneous ground, or an existing cavity may create an initial weak state. Seepage associated with pipeline damage, rainfall infiltration, traffic loading, or lateral displacement may then promote the migration of water and soil or the accumulation of deformation. At C01, the available conditions are compatible with a sequence involving construction disturbance followed by damage to a branch pipe. At C10, deterioration of support associated with pipeline damage may also be amplified by traffic loading. By contrast, the contribution of rainfall at C08 and the presence of an initial weak zone at C09 have not been directly verified.

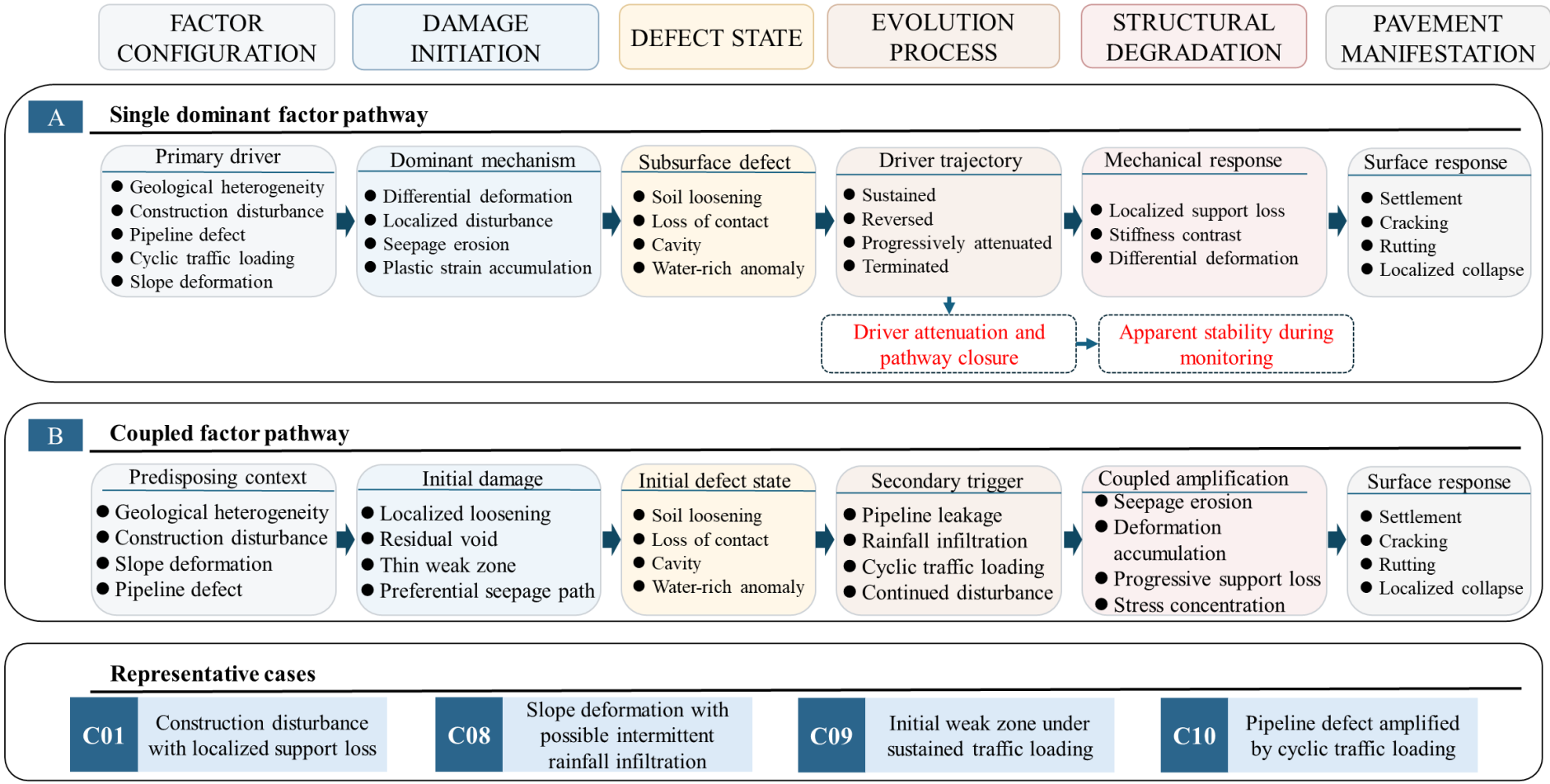


Fig. 10 Conceptual stage-specific failure pathways of shallow subsurface defects beneath urban roads governed by a single dominant factor or interacting factors

Figure 10 provides a conceptual framework for organizing evidence from multiple sources rather than a representation of continuously observed stages. The available data cannot establish the exact timing of factor activation, the independent contribution of each factor, or the threshold for failure. The framework therefore supports only conditional mechanistic interpretations and should not be regarded as a validated deterministic causal model.

4.5 Performance degradation and resilience of road systems affected by subsurface defects

Infrastructure resilience refers to the ability of a system to maintain essential functions and limit performance loss under disturbance, and to restore its service capacity through adaptation or repair [23, 24]. For the pavement structure and underlying ground considered in this study, resilience is reflected in the ability of the road system to maintain safety and basic traffic function when subsurface support deteriorates, moisture conditions change, differential deformation develops, or cyclic loading persists. It also includes the ability to restore structural performance and serviceability after engineering intervention. Road resilience therefore encompasses both structural bearing and deformation performance and the recovery of traffic function and service level [25].

The presence of subsurface soil loosening, loss of contact, or cavities does not in itself indicate that the road has failed. During the early stage of defect development, the overlying pavement and surrounding ground may continue to maintain basic function through their remaining bearing capacity, load redistribution, and deformation compatibility. As the defect continues to expand, local loss of support and stiffness contrasts may exceed the remaining capacity of the pavement structure and its ability to accommodate differential deformation. Subsurface anomalies may then progressively manifest as surface settlement, rutting, cracking, and lateral displacement. These responses and corresponding differences in FWD measurements were observed in the investigated cases, indicating that subsurface defects had affected the structural performance of some road sections. However, the available evidence is insufficient to determine whether their bearing or deformation limit states had been reached. In terms of failure progression, subsurface defects may initially cause serviceability degradation, including reduced ride quality, rutting, localized settlement, and cracking. If the causative source remains active or the action pathway remains open, continued deterioration may result in local loss of support beneath the base course, plastic deformation of the subgrade, and reduced bearing capacity. The road may consequently progress from serviceability degradation to structural failure. For shallow cavities accompanied by continued soil loss, localized pavement collapse is a possible conditional consequence. In slope and embankment systems affected by persistent lateral displacement, localized instability may also occur. More severe functional and secondary consequences may include lane closure, traffic disruption, damage to adjacent utilities, and risks to road users. However, these consequences were not directly observed in the investigated cases.

Road resilience depends not only on the performance retained by the road system after defect formation but also on the persistence of the causative source, the state of the action pathway, and the timing and effectiveness of remediation. If the causative source weakens, the action pathway closes, and stable support can be re-established, the defect may enter a temporarily stable state. If pipeline defects, slope displacement, or heavy traffic loading persist, structural performance may continue to deteriorate, increasing both the difficulty of subsequent repair and the time required to restore function. No subsurface anomaly was identified at C06 after pavement rehabilitation, indicating that engineering intervention can alter the defect state. However, continuous performance records, the extent of functional loss, and the time required for recovery were unavailable. This case therefore cannot be used to calculate a resilience metric. Similarly, limited geometric changes in the other cases cannot be interpreted as evidence of high resilience. This study consequently provides only a qualitative assessment of defect formation, performance degradation, and the conditions required for engineering recovery. It does not assign resilience levels or quantitatively evaluate resilience for the individual cases.

5 Discussion

The preceding analyses indicate that the causes responsible for initial defect formation, defect activity during the observation interval, and the performance response of the pavement structure represent three interrelated but distinct levels of analysis. Investigations based on multiple sources of evidence can increase confidence in causal interpretations, while comparison of the initial and repeat surveys can identify apparent changes in defect condition. However, neither approach can directly determine how a defect will evolve over the long term, when structural failure will occur, or the level of road resilience. This chapter therefore discusses the relationship between the present findings and previous studies, changes in the roles of multiple factors across different stages, management implications for defect activity and resilience restoration, and the applicability and limitations of the conclusions.

5.1 Relationship between the present findings and previous studies

Previous studies of urban road collapse have commonly used accident databases to identify factors such as pipe damage, construction disturbance, adverse geological conditions, and intense rainfall [1, 2]. Studies on the management of subsurface cavities beneath roads have focused mainly on defect detection, severity classification, and repair performance [3]. Physical model tests and numerical simulations have further clarified the basic processes of water and soil migration, cavity expansion, and surface deformation in the presence of pipe defects [6, 8, 18, 22]. These studies demonstrate the failure processes that may result from different causative factors. However, they generally cannot establish which factor dominates a specific field defect or whether the corresponding process remains active during a particular observation interval.

At the scale of individual cases, the present study shows that causal attribution cannot be based solely on anomaly type or the spatial proximity of a potential causative factor. At C10, the pipe damage, zone of severe soil loosening, surface deformation, and FWD response exhibited consistent spatial correspondence. Together, these observations formed a relatively complete chain of evidence for internal erosion associated with pipe damage. By contrast, relevant pipe defects at C03–C05 and C07 were remote from the anomalies, absent, or incompatible with them in elevation. Geological heterogeneity therefore provided a stronger explanation for these cases. No drainage pipe capable of explaining the extensive soil loosening was identified beneath the traffic lane at C09. Prolonged heavy traffic and the corresponding pavement response thus provided a more plausible explanation. Field attribution therefore requires consistency among the causative source, location of action, and expected process. Negative evidence is also needed to discount alternative explanations with weaker explanatory power.

In this study, GPR, borehole investigation, FWD testing, and pipeline CCTV inspection respectively characterized anomaly geometry, local material conditions, pavement structural response, and potential causative sources. Their complementary roles are consistent with previous studies of nondestructive investigation [13, 15]. The results further show that anomaly area, depth to the top boundary, equivalent thickness, and anomaly type do not necessarily change synchronously. At C02, contraction of the cavity core coincided with increased thickness and peripheral soil loosening. C03 and C07 exhibited apparent vertical changes despite little or no change in anomaly area. C08 and C09 showed different forms of horizontal expansion. These findings indicate that anomaly type and geometric extent at a single survey mainly describe the current defect state. A conditional assessment of defect activity requires consideration of changes between surveys, persistence of the causative source, and the corresponding pavement response.

5.2 Changes in the roles of multiple factors and external amplifying conditions

The results indicate that natural and anthropogenic factors interact during defect development, and that their relative contributions and dominant roles may change across different stages. Geological heterogeneity primarily controls the locations susceptible to defect formation and the initial support conditions. Construction disturbance may create residual voids or loosened zones. Pipe defects can maintain pathways for the migration of water and soil. Slope displacement and cyclic traffic loading may further amplify existing nonuniformity in ground support. Different factors may therefore become involved sequentially and affect subsequent defect conditions by changing seepage, deformation, or load transfer.

This stage dependent interpretation helps explain why the attributed cause and the observed pattern of change do not always correspond directly. The principal geometric indicators at C04 and C10 remained relatively stable during the observation interval. However, C04 retained its background of weak and heterogeneous ground, while the pipe defect and potential migration pathway at C10 had not been eliminated. Geometric stability therefore does not demonstrate that the causative process has ceased. The anomaly extents at C08 and C09 increased, suggesting that relevant driving conditions may have remained active. Nevertheless, the available evidence is insufficient to confirm that the observed expansion was caused entirely by the continued action of the originally attributed factor. Attribution of the initial cause explains how a defect may have formed. Assessment of its subsequent activity additionally requires examination of whether the causative source, action pathway, and external disturbances remain active.

Climatic and hydrological conditions may modify the intensity of these processes. Studies of climate change and related research in Shanghai suggest that the risks associated with extreme precipitation, design rainstorms during typhoon events, and the combined effects of rainfall and storm surge may change [26, 30]. Accident statistics and numerical studies also indicate that repeated intense rainfall may increase the risks of underground infrastructure failure and road collapse when infrastructure defects, pathways for particle migration, and adverse geological conditions coexist [31, 32]. Internal erosion associated with pipe damage is also governed by defect geometry, hydraulic gradient, and the conditions controlling soil discharge [33, 34]. Cumulative deformation under traffic loading depends on soil water content, cycles of wetting and drying, and the remaining bearing capacity [35, 36].

For the investigated cases, intense rainfall may aggravate slope and embankment deformation at C08, enhance the migration of water and soil near C01 and C10, and reduce the remaining performance capacity of the weakened subgrade at C09 under cyclic loading. However, rainfall, groundwater level, pore water pressure, and soil water content were not monitored concurrently with the repeat surveys. The actual contribution of climatic and hydrological conditions to each case therefore cannot be verified. These factors can only be regarded as possible triggers or amplifying conditions. They cannot be used to revise the attribution of the principal cause or to infer that climate change has already accelerated the development of the investigated defects.

5.3 Management implications for defect activity and resilience restoration

Conventional defect remediation commonly determines priorities according to anomaly type, area, or cover depth. The present findings show, however, that geometric extent and defect activity are not always consistent. A small or temporarily stable defect may present greater subsequent risk than a larger residual anomaly if its causative source remains active and its action pathway remains open. Management should therefore address not only the anomaly itself but also its causative source, action pathway, and the response of the pavement structure.

A road may retain basic traffic service under routine loading while its remaining bearing capacity has not been exhausted. This condition does not demonstrate that the subsurface defect is stable or that the road has high resilience. Intense rainfall, changes in soil water content, continued heavy traffic, or slope displacement may further reduce the remaining performance capacity. Local deterioration of support may then develop rapidly into settlement, cracking, or interruption of service. The central objective of management is therefore to prevent the defect from crossing the threshold of structural failure under external disturbance and to restore bearing capacity and traffic service promptly after performance loss. Corresponding management measures should control persistent causative sources, interrupt pathways for water and soil migration or deformation transfer, restore uniform support beneath the pavement, and verify remediation performance through repeat surveys. At C10, priority should be given to repairing the pipe defect and examining the hydraulic connection between the inside and outside of the pipe. At C08, drainage conditions, slope displacement, and embankment deformation should be managed in an integrated manner. At C09, traffic load management, drainage conditions, and subgrade bearing performance should all be considered. No subsurface anomaly was identified at C06 after pavement rehabilitation, indicating that engineering intervention can alter defect condition. However, the absence of continuous performance records and recovery time data prevents evaluation of its resilience over the long term.

Priorities for repeat surveys should be determined jointly by defect activity and the remaining performance capacity of the pavement. Particular attention should be given to sites where the causative source persists, the action pathway remains open, the anomaly extent increases, the top boundary moves toward the ground surface, or a clear pavement response has already developed. Regional susceptibility and risk zoning can help identify priority areas for investigation [37], but cannot replace examination of causative sources, action pathways, and structural responses at individual sites.

5.4 Applicability, limitations, and directions for further research

The proposed evidence chain and stage based interpretation framework are primarily applicable to urban roads in coastal soft ground characterized by heterogeneous shallow fill, dense underground utility networks, and intensive traffic activity. Karst terrain, former mining areas, deep underground construction, and regional land subsidence involve substantially different causative conditions, spatial scales, and failure processes. The conclusions of this study should not be transferred directly to these settings. They are intended as conditional interpretations at the scale of individual cases and should not be used to calculate regional proportions of causes, failure probabilities, or risk distributions.

This study has three principal limitations. First, although similar investigation procedures were adopted in the initial and repeat surveys, the interpreted boundaries of GPR anomalies may still have been affected by soil water conditions, interpretation thresholds, and errors in reproducing survey lines. The minimum detectable change was not quantified. Moreover, two survey campaigns are insufficient to estimate rates of defect development or determine stability over the long term. Second, continuous records of rainfall, groundwater level, water level inside the pipes, pore water pressure, soil water content, vehicle axle loads, and surface deformation were unavailable. The independent contributions of hydraulic action, traffic loading, and ground deformation could therefore not be quantified. The exact sequence in which these factors became involved also remains uncertain. Finally, particle migration, pore evolution, and damage to soil structure were interpreted mainly from previous studies and were not directly verified through controlled experiments in the present study. Continuous records of performance loss, repair duration, and restoration of service function were also unavailable. The study can therefore discuss only resilience responses and the conditions required for recovery. It cannot calculate resilience metrics or assign resilience levels.

Future studies should conduct coordinated monitoring over multiple periods along road sections affected by pipe damage, slope deformation, and heavy traffic. GPR survey lines, interpretation criteria, and verification locations should be standardized. Rainfall, groundwater level, water level inside pipes, pore water pressure, soil water content, axle loads, and surface deformation should be analyzed together with CCTV inspection and FWD measurements. Internal erosion tests, cyclic loading tests, and coupled hydro-mechanical simulations could then be used to verify the proposed failure pathways and identify the conditions governing transitions from temporary stability to continued development or structural failure. Continuous indicators should also be established to characterize pavement performance loss, engineering intervention, and restoration of service function, thereby providing a basis for quantitative resilience assessment.

6 Conclusions

This study investigated ten shallow subsurface defects beneath urban roads in a coastal area underlain by soft soils. Evidence from GPR, borehole investigations and pavement coring, FWD testing, CCTV inspection of drainage pipes, utility detection, historical records, and field reconnaissance was integrated to examine causal attribution at the case scale, apparent changes between two survey campaigns, potential failure pathways, and pavement performance degradation and resilience responses. The principal conclusions are as follows.

(1) Different investigation methods characterize distinct dimensions of evidence for subsurface defects. GPR primarily delineates anomaly geometry and depth. Borehole investigations and pavement coring verify local material conditions and structural state. Pipeline CCTV inspection, utility detection, and historical records help identify potential causative sources and action pathways. FWD testing and surface

investigation characterize pavement structural responses. Reliable causal attribution requires examination of whether candidate factors are compatible with the observed defects in spatial location, relevant elevation, and expected process. Evidence from multiple sources should be considered together, while negative evidence should be used to test alternative explanations. An isolated anomaly, spatial proximity to a potential causative factor, or the result of a single investigation method is insufficient to establish the cause of a defect.

(2) Under the available evidence, C03, C04, C05, and C07 are more strongly supported by explanations involving geological heterogeneity, while C08 shows a close spatial correspondence with slope and embankment deformation. C01 and C02 are more consistent with residual loosened zones or voids caused by trenchless construction disturbance. C09 is better explained by cumulative deformation under prolonged heavy traffic. C10 is consistent with internal erosion caused by groundwater-driven soil migration into the pipe through a pipe defect. C06 had undergone pavement rehabilitation before the repeat survey, after which no anomaly was identified. However, the post-intervention condition cannot be used to infer the original cause, and no definitive attribution was therefore made. These interpretations represent the relative support for different explanations under the current evidence. They do not exclude the involvement of underlying conditions or interacting factors and cannot be extrapolated to represent the relative frequencies of different causes across the study area.

(3) Except for C06, the comparison between the two survey campaigns for the remaining nine cases revealed horizontal expansion, vertical changes, changes in anomaly type combinations, relative geometric stability, and mixed changes involving multiple indicators. At C08, the zone of severe soil loosening expanded and was accompanied by a shallower top boundary, increased thickness, and localized loss of contact, indicating combined horizontal and vertical changes. C09 mainly exhibited horizontal expansion of severe soil loosening. C03 and C07 showed apparent vertical changes despite no change in anomaly area. At C02, the cavity core contracted markedly, but the simultaneous increase in thickness and development of peripheral general soil loosening do not indicate overall defect regression. Although the relative increase in thickness at C05 was large, the absolute increase was only 0.20 m and is insufficient to demonstrate marked defect progression. The principal geometric indicators at C04 and C10 remained relatively stable during the observation interval, but this does not demonstrate that the corresponding causative processes had ceased. Defect condition should therefore be assessed by jointly considering anomaly area, depth to the top boundary, vertical thickness, anomaly type, and causative conditions. No single indicator can adequately characterize the overall change in defect condition.

(4) Different causative factors may weaken support beneath the pavement through differential deformation, construction-induced loosening, internal erosion, plastic strain accumulation under cyclic loading, and lateral deformation of slopes and embankments. Natural and anthropogenic factors may interact during defect development, and their relative contributions may change across different stages. Geological heterogeneity or construction disturbance may create susceptible zones and initial defects, while subsequent hydraulic action, traffic loading, or lateral displacement may sustain or amplify the existing damage. This stage-based interpretation provides a framework for organizing field evidence and identifying monitoring priorities. However, the available data are insufficient to determine the exact sequence in which individual factors became involved or to quantify their independent contributions. They also cannot support calculation of defect development rates, failure probabilities, or the timing of failure.

(5) The presence of subsurface soil loosening, loss of contact, or cavities does not necessarily indicate that the road structure has already failed. During the early stages of defect development, the overlying pavement and surrounding ground may retain basic traffic function through their remaining bearing capacity, load redistribution, and deformation compatibility. When local support deterioration and stiffness contrasts exceed the remaining structural capacity and the ability of the pavement to accommodate differential deformation, subsurface anomalies may develop into settlement, rutting, cracking, lateral displacement, and reduced bearing performance. Pavement responses and spatial variations in FWD measurements were observed in several cases, but the available evidence is insufficient to determine whether structural failure thresholds had been reached. Maintaining and restoring road resilience require control of persistent causative sources, interruption of pathways for water and soil migration or deformation transfer, restoration

of uniform structural support, and verification of remediation performance through repeat surveys. C06 demonstrates that engineering intervention can alter defect condition. However, because continuous records of performance loss and recovery time were unavailable, this study provides only a qualitative analysis of pavement performance degradation and the conditions required for recovery. It cannot calculate resilience metrics or assign resilience levels.

Author contributions

Hongbo Zhou and Rongxin Zhao conceived and designed the study and managed the project. Yian Wang conducted the field investigation and reviewed and edited the manuscript. Yinbing Cui curated and analyzed the data and prepared the first draft of the manuscript.

Funding

This research was supported by the National Key Research and Development Program of China (Grant No. 2023YFC3807604).

Data availability

The data supporting the findings of this study are available from the corresponding author upon reasonable request.

Declarations

Ethics and consent to participate

Not applicable.

Competing interests

The authors declare no competing interests.

References

1. Tan Y, Long YY (2021) Review of cave-in failures of urban roadways in China: A database. Journal of Performance of Constructed Facilities 35(6):04021080
2. Wang K, Zhang JW, Gao GQ, et al (2022) Causes, risk analysis, and countermeasures of urban road collapse in China from 2019 to 2020. Journal of Performance of Constructed Facilities 36(6):04022054
3. Lee S, Park JJ, Cho BH (2022) Management of cavities under flexible pavement road network in metropolitan area: Detection, evaluation, and rehabilitation. Developments in the Built Environment 12:100091
4. Chai JC, Miura N (2002) Traffic-load-induced permanent deformation of road on soft subsoil. Journal of Geotechnical and Geoenvironmental Engineering 128(11):907-916
5. Cui X, Zhang N, Zhang J, Gao Z (2014) In situ tests simulating traffic-load-induced settlement of alluvial silt subsoil. Soil Dynamics and Earthquake Engineering 58:10-20
6. Zhang DM, Du WW, Peng MZ, Feng SJ, Li ZL (2020) Experimental and numerical study of internal erosion around submerged defective pipe. Tunnelling and Underground Space Technology 97:103256
7. Guo S, Shao Y, Zhang T, Zhu DZ, Zhang Y (2013) Physical modeling on sand erosion around defective sewer pipes under the influence of groundwater. Journal of Hydraulic Engineering 139(12):1247-1257
8. Indiketiya S, Jegatheesan P, Rajeev P, Kuwano R (2019) The influence of pipe embedment material on sinkhole formation due to erosion around defective sewers. Transportation Geotechnics 19:110-125
9. Lan H, Yan X, Moore ID (2024) Mud infiltration and travel paths during mud loss experiments on horizontal borehole stability. Tunnelling and Underground Space Technology 144:105565

10. Ahmed A, Islam MA, Alam MZ, Quazi HS (2023) Surface settlement induced by horizontal directional drilling. Underground Space 8:94-108

11. Oh WT, Vanapalli SK (2010) Influence of rain infiltration on the stability of compacted soil slopes. Computers and Geotechnics 37(5):649-657

12. Zheng Y, Wu H, Luan X, McCartney JS (2024) Numerical simulation of rainfall-induced deformations of embankments considering the coupled hydro-mechanical behavior of unsaturated soils. Computers and Geotechnics 175:106714

13. Chen DH, Wimsatt A (2010) Inspection and condition assessment using ground penetrating radar. Journal of Geotechnical and Geoenvironmental Engineering 136(1):207-214

14. Bianchini Ciampoli L, D'Amico F, Tosti F, Alani AM, Benedetto A (2018) An experimental-based model for the assessment of the mechanical properties of road pavements using ground-penetrating radar. Construction and Building Materials 165:966-974

15. Marecos V, Fontul S, Antunes ML, Solla M (2017) Evaluation of a highway pavement using non-destructive tests: Falling Weight Deflectometer and Ground Penetrating Radar. Construction and Building Materials 154:1164-1172

16. Peduto D, Giangreco C, Venmans AAM (2020) Differential settlements affecting transition zones between bridges and road embankments on soft soils: Numerical analysis of maintenance scenarios by multi-source monitoring data assimilation. Transportation Geotechnics 24:100369

17. Prosperi A, de Gast T, Korswagen PA, Korff M, Rots JG (2025) Lithological heterogeneity and its impact on soil settlements at the building scale. Geotechnical and Geological Engineering 43:206

18. Sato M, Kuwano R (2015) Influence of location of subsurface structures on development of underground cavities induced by internal erosion. Soils and Foundations 55(4):829-840

19. Kwak TY, Woo SI, Kim J, Chung CK (2019) Model test assessment of the generation of underground cavities and ground cave-ins by damaged sewer pipes. Soils and Foundations 59(3):586-600

20. Mukunoki T, Kumano N, Otani J, Kuwano R (2009) Visualization of three dimensional failure in sand due to water inflow and soil drainage from defective underground pipe using X-ray CT. Soils and Foundations 49(6):959-968

21. Indiketiya S, Jegatheesan P, Rajeev P (2017) Evaluation of defective sewer pipe-induced internal erosion and associated ground deformation using laboratory model test. Canadian Geotechnical Journal 54:1184-1195

22. Guo S, Zhu DZ (2017) Soil and groundwater erosion rates into a sewer pipe crack. Journal of Hydraulic Engineering 143(7):06017008

23. Bruneau M, Chang SE, Eguchi RT, et al (2003) A framework to quantitatively assess and enhance the seismic resilience of communities. Earthquake Spectra 19(4):733-752

24. Francis R, Bekera B (2014) A metric and frameworks for resilience analysis of engineered and infrastructure systems. Reliability Engineering & System Safety 121:90-103

25. Matini N, Gulzar S, Underwood S, et al (2022) Evaluation of structural performance of pavements under extreme events: Flooding and heatwave case studies. Transportation Research Record 2676(7):233-248

26. IPCC (2021) Climate Change 2021: The Physical Science Basis. Cambridge University Press, Cambridge

27. Knutson T, Camargo SJ, Chan JCL, et al (2020) Tropical cyclones and climate change assessment: Part II—Projected response to anthropogenic warming. Bulletin of the American Meteorological Society 101(3):E303-E322

28. Mou Y, Gao X, Yang Z, et al (2022) Variation characteristics and the impact of urbanization of extreme precipitation in Shanghai. Scientific Reports 12:17618

29. Jin Y, Liu S, Zhou Z, et al (2024) The influence of typhoon events on the design storm for the Shanghai metropolitan area in the Yangtze River Delta, China. Water 16(3):508

30. Xu H, Ragno E, Jonkman SN, et al (2024) Combining statistical and hydrodynamic models to assess compound flood hazards from rainfall and storm surge: A case study of Shanghai. Hydrology and Earth System Sciences 28(16):3919-3930

31. Jiang W, Tan Y (2022) Overview on failures of urban underground infrastructures in complex geological conditions due to heavy rainfall in China during 1994-2018. Sustainable Cities and Society 76:103509

32. Jung B, Ryu DW, Yum BW (2023) Numerical simulation of urban road collapse induced by the damaged sewer pipe and repetitive heavy rainfalls. Geosciences Journal 27:515-529

33. Cao L, Li X, Li Z, et al (2024) Influence of drainage flow velocity on microscopic cohesive soil erosion and macroscopic road collapse evolution: A case study in Beijing, China. Engineering Failure Analysis 164:108698

34. Guo J, Zhang Y, Cheng Y, et al (2025) Study on urban ground collapse induced by defective pipelines based on physical model experiments and numerical simulation. Scientific Reports 15:6085

35. Lu Z, Fang R, Chen LH, et al (2020) Long-term deformation of highway subgrade under coupling effect of traffic load and drying-wetting cycles. International Journal of Geomechanics 20(2):04019168

36. Thevakumar K, Indraratna B, Ferreira FB, et al (2021) The influence of cyclic loading on the response of soft subgrade soil in relation to heavy haul railways. Transportation Geotechnics 29:100571

37. Zhang Y, Jiao YY, He LL, et al (2024) Susceptibility mapping and risk assessment of urban sinkholes based on grey system theory. Tunnelling and Underground Space Technology 152:105893